Title

Lipoxins reduce obesity-induced adipose tissue inflammation in 3D-cultured human adipocytes and explant cultures

Journal

iScience, 25(7)

ISSN

2589-0042

Authors

Soták, Matúš
Rajan, Meenu Rohini
Clark, Madison
et al.

Publication Date

2022-07-01

DOI

10.1016/j.isci.2022.104602

Peer reviewed

iScience

CellPress
OPEN ACCESS

Article

Lipoxins reduce obesity-induced adipose tissue inflammation in 3D-cultured human adipocytes and explant cultures

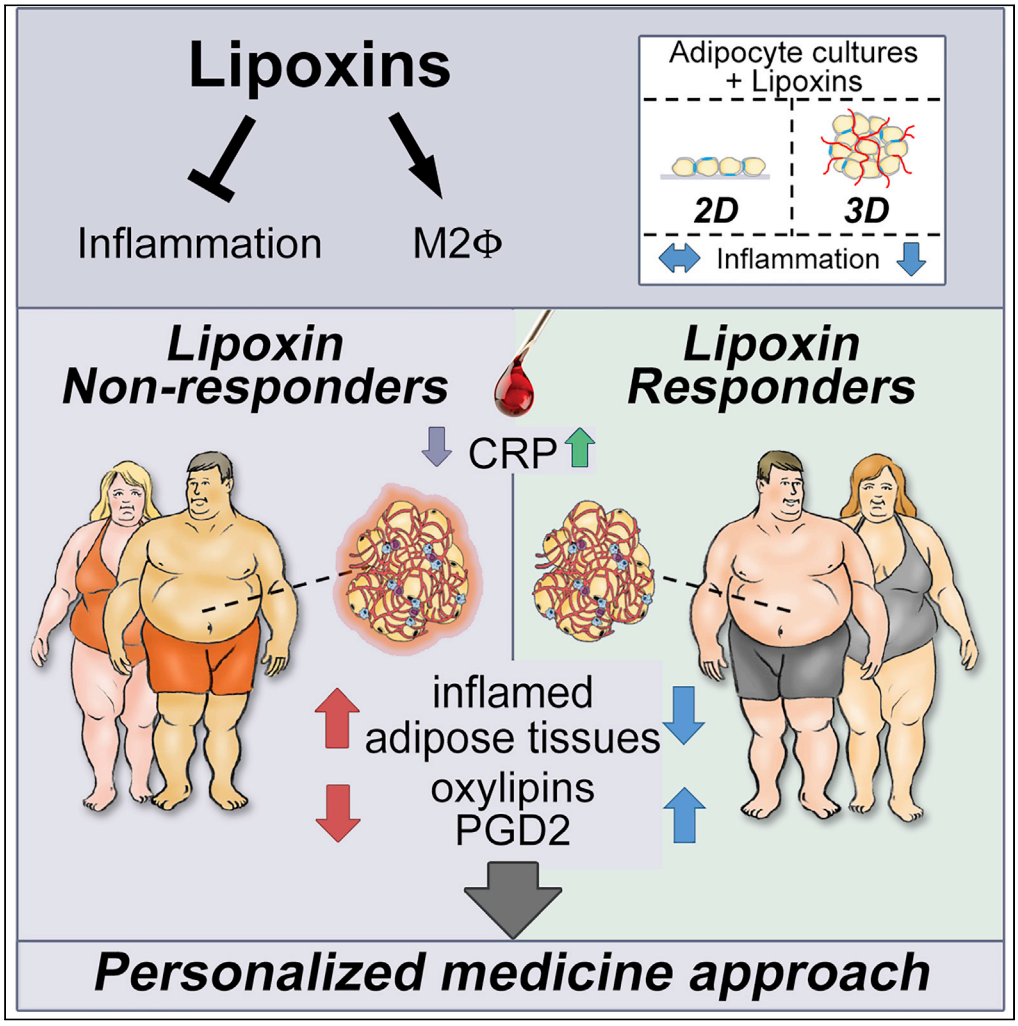

Matúš Soták, Meenu Rohini Rajan, Madison Clark, ..., Ville Wallenius, Stephan Lange, Emma Börgeson

emma.borgeson@wlab.gu.se

Highlights

3D cell culture systems amplify lipoxin-mediated responses in human adipocytes

Lipoxins reduce obesity-related inflammation in human adipose tissue explants

The amplitude of a lipoxin-mediated response correlates with a patient's plasma CRP level

Lipoxin responders have altered inflammatory and adipose tissue lipid profiles

Soták et al., iScience 25, 104602
July 15, 2022
https://doi.org/10.1016/j.isci.2022.104602

iScience

CellPress
OPEN ACCESS

Article

Lipoxins reduce obesity-induced adipose tissue inflammation in 3D-cultured human adipocytes and explant cultures

Matúš Soták,[1,2,3,15] Meenu Rohini Rajan,[1,2,3,15] Madison Clark,[1,2] Matthew Harms,[13] Alankrita Rani,[1,2,3] Jamie D. Kraft,[1,2] David Tandio,[1,2] Tong Shen,[5] Kamil Borkowski,[5] Oliver Fiehn,[5] John W. Newman,[5,6,7] Marianne Quiding-Järbrink,[8] Christina Biörserud,[9] Peter Apelgren,[9,10] Trude Staalesen,[9,10] Carolina E. Hagberg,[11,12] Jeremie Boucher,[2,4,13] Ville Wallenius,[9] Stephan Lange,[1,14] and Emma Börgeson[1,2,3,16,*]

SUMMARY

Adipose tissue inflammation drives obesity-related cardiometabolic diseases. Enhancing endogenous resolution mechanisms through administration of lipoxin A_4, a specialized pro-resolving lipid mediator, was shown to reduce adipose inflammation and subsequently protects against obesity-induced systemic disease in mice. Here, we demonstrate that lipoxins reduce inflammation in 3D-cultured human adipocytes and adipose tissue explants from obese patients. Approximately 50% of patients responded particularly well to lipoxins by reducing inflammatory cytokines and promoting an anti-inflammatory M2 macrophage phenotype. Responding patients were characterized by elevated systemic levels of C-reactive protein, which causes inflammation in cultured human adipocytes. Responders appeared more prone to producing anti-inflammatory oxylipins and displayed elevated prostaglandin D2 levels, which has been interlinked with transcription of lipoxin-generating enzymes. Using explant cultures, this study provides the first proof-of-concept evidence supporting the therapeutic potential of lipoxins in reducing human adipose tissue inflammation. Our data further indicate that lipoxin treatment may require a tailored personalized-medicine approach.

INTRODUCTION

Obesity-related cardiometabolic diseases are fueled by adipose tissue and low-grade systemic inflammation (Börgeson and Sharma, 2013; Henning, 2021). Drugs targeting pro-inflammatory pathways have therefore been suggested as a therapeutic strategy to reduce cardiometabolic pathophysiology (Donath et al., 2013). Clinical trials have demonstrated the promising potential of this approach (Nidorf et al., 2020; Ridker et al., 2017; Stanley et al., 2011; Tardif et al., 2019). However, traditional anti-inflammatory therapies may have serious side effects, such as increased susceptibility to infections. Therefore, specialized pro-resolving mediators (SPMs) that enhance endogenous resolution mechanisms were suggested as an alternative strategy (Panigrahy et al., 2021; Serhan and Levy, 2018).

Endogenously produced SPMs regulate the active process of inflammatory resolution (Serhan and Levy, 2018). SPMs include ω-6 arachidonic acid-derived lipoxins, and ω-3 eicosapentaenoic and docosahexaenoic acid-derived resolvins, protectins and maresins (Serhan et al., 2020). Mechanistically, SPMs initiate the resolution of inflammation by halting neutrophil recruitment and reducing pro-inflammatory cytokines, while promoting recruitment of nonphlogistic monocytes, an M1-to-M2 macrophage phenotype switch, and the removal of dead cells (efferocytosis) (Godson et al., 2000; Panigrahy et al., 2021). SPMs may also terminate the inflammatory response by promoting immune cell egression through the lymphatics (Kraft et al., 2021). Interestingly, obese individuals may have an impaired ability to resolve low-grade inflammation due to an imbalance of SPMs and pro-inflammatory factors (Lopez-Vicario et al., 2019).

We previously demonstrated that lipoxins reduce adipose inflammation and obesity-induced organ injury in mice (Börgeson et al., 2012, 2015). Lipoxins comprise of two main members: Lipoxin A_4 (LXA_4) and

[1]Department of Molecular and Clinical Medicine, Wallenberg Laboratory, Institute of Medicine, Sahlgrenska Academy, University of Gothenburg, 40530 Gothenburg, Sweden

[2]Wallenberg Centre for Molecular and Translational Medicine, University of Gothenburg, 40530 Gothenburg, Sweden

[3]Region Vaestra Goetaland, Sahlgrenska University Hospital, Department of Clinical Physiology, 41345 Gothenburg, Sweden

[4]The Lundberg Laboratory for Diabetes Research, Department of Molecular and Clinical Medicine, Sahlgrenska Academy, University of Gothenburg, Gothenburg, Sweden

[5]NIH West Coast Metabolomics Center, Genome Center, University of California Davis, Davis, CA 95616, USA

[6]Department of Nutrition, University of California Davis, Davis, CA 95616, USA

[7]USDA, ARS, Western Human Nutrition Research Center, Davis, USA

[8]Department of Microbiology and Immunology, Institute of Biomedicine, Sahlgrenska Academy, University of Gothenburg, 40530 Gothenburg, Sweden

[9]Department of Surgery, Institute of Clinical Sciences, Sahlgrenska Academy, University of Gothenburg, Gothenburg, Sweden

[10]Region Vaestra Goetaland, Sahlgrenska University Hospital, Department of

Continued

Lipoxin B_4 (LXB_4). On cultured mouse adipocytes, LXA_4 promoted glucose uptake, attenuated pro-inflammatory cytokines, and stimulated other anti-inflammatory mediators (Börgeson et al., 2012). LXA_4 also prevented obesity-induced diabetes and organ injury in mice by promoting an M1-to-M2 macrophage phenotype switch, attenuating adipose tissue inflammation, and subsequent disease development in an adiponectin-independent manner (Börgeson et al., 2015). Effects of LXB_4 are mostly unknown and remain to be elucidated. Although SPMs are readily detectable in human adipose tissue (Claria et al., 2013), it is still not known whether lipoxin administration could reduce adipose tissue inflammation in humans.

Here, we translate our previous findings to human pathophysiology and investigate the therapeutic potential of lipoxins in reducing human adipose tissue inflammation. We use patient-specific explants from obese patients, as well as 2D- and 3D human adipocyte cell culture models to investigate lipoxin-mediated effects on inflammatory resolution.

RESULTS

Lipoxins require a 3D environment to robustly attenuate inflammation in cultured human adipocytes

We compared lipoxin-mediated effects in differentiated adipocytes cultured in 2D- and 3D models (Figure 1A). Cells obtained from adipose tissue of obese patients (body mass index (BMI) > 30 kg/m^2) undergoing abdominoplasty surgery were used for 2D- and 3D membrane mature adipocyte aggregate culture (MAAC) cell culture. We also used the human unilocular vascularized adipocyte spheroid (HUVAS) 3D culture spheroid system (Ioannidou et al., 2021) with commercially available primary human stromovascular cells.

Lipoxin-mediated effects were mild or absent in adipocytes grown in 2D cultures, where we only observed an attenuation of interleukin (IL)-6 levels following LXB_4 treatment (Figure 1B). Adipocytes isolated from the same donor but cultured in the 3D MAAC model showed lipoxin-induced reductions in the expression of pro-inflammatory cytokines, including IL-8, IL-6, TNF-α, and IL-1β (Figure 1C). The 3D HUVAS spheroids showed the strongest lipoxin-mediated effects, with both lipoxins decreasing all screened inflammatory cytokines (Figure 1D).

In summary, both lipoxins were able to robustly reduce inflammation in 3D cultures, while lipoxin-mediated effects were mild or absent in 2D-cultured adipocytes.

Lipoxins reduce obesity-related inflammation in human adipose tissue explants from patients with elevated CRP levels

Next, we wondered if lipoxins could attenuate adipose tissue inflammation in a model that better reflects the patient's intact adipose tissue. Instead of isolating cells for subsequent cell culture, we used adipose tissue explants from obese gastric bypass patients (BMI $\geq$40, or BMI $\geq$35 with $\geq$1 co-morbidity). The explant cultures were restricted to 6 h (Figure 2A), which limits the occurrence of hypoxia (Börgeson et al., 2012). Subsequently, expression levels of inflammatory and resolving markers were measured.

Lipoxins affected inflammatory and pro-resolving pathways differently in two patient subgroups, which were subsequently referred to as non-responders and responders. Briefly, ~50% of patients responded to lipoxin treatment, which was determined as a significant upregulation of the lipoxin-regulated M2 macrophage marker CD206 (Börgeson et al., 2015). Screening of clinical parameters revealed that responders also exhibited elevated levels of C-reactive protein (CRP). Therefore, the clinically relatable cut-off criteria for elevated CRP of $\geq$5 mg/L was used to separate responders and non-responders, as opposed to CD206 levels which is not typically available in the clinic (see STAR Methods). Besides elevated CRP, both groups had comparable clinical phenotypes, showing no difference in age or adiposity (Table 1).

Metabolic disorders change the number and phenotype of macrophages in peripheral organs, including adipose tissues. The accumulation of macrophages correlates with tissue inflammation and fibrosis, contributing to the disease progression (Olefsky and Glass, 2010). LXA_4 protects against metabolic disease in rodents by reducing TNF-α and promoting an M1-to-M2 macrophage phenotype switch (Börgeson et al., 2015). Thus, we investigated levels of anti-inflammatory (CD206, CD163) and pro-inflammatory (CD11c) macrophages in adipose explants from responders and non-responders. In responders, both lipoxins increased *MRC1* (coding for CD206) and *CD163* mRNA levels (Figures 2B and 2C), suggesting an active

Plastic Surgery, Gothenburg, Sweden

[11]Division of Cardiovascular Medicine, Department of Medicine Solna, Karolinska Institutet, Stockholm, Sweden

[12]Center for Molecular Medicine, Karolinska Institutet, Stockholm, Sweden

[13]Bioscience Metabolism, Research and Early Development, Cardiovascular, Renal and Metabolism (CVRM), BioPharmaceuticals R&D, AstraZeneca, Gothenburg, Sweden

[14]Division of Cardiology, School of Medicine, University of California San Diego, San Diego, CA, USA

[15]These authors contributed equally

[16]Lead contact

*Correspondence: emma.borgeson@wlab.gu.se

https://doi.org/10.1016/j.isci.2022.104602

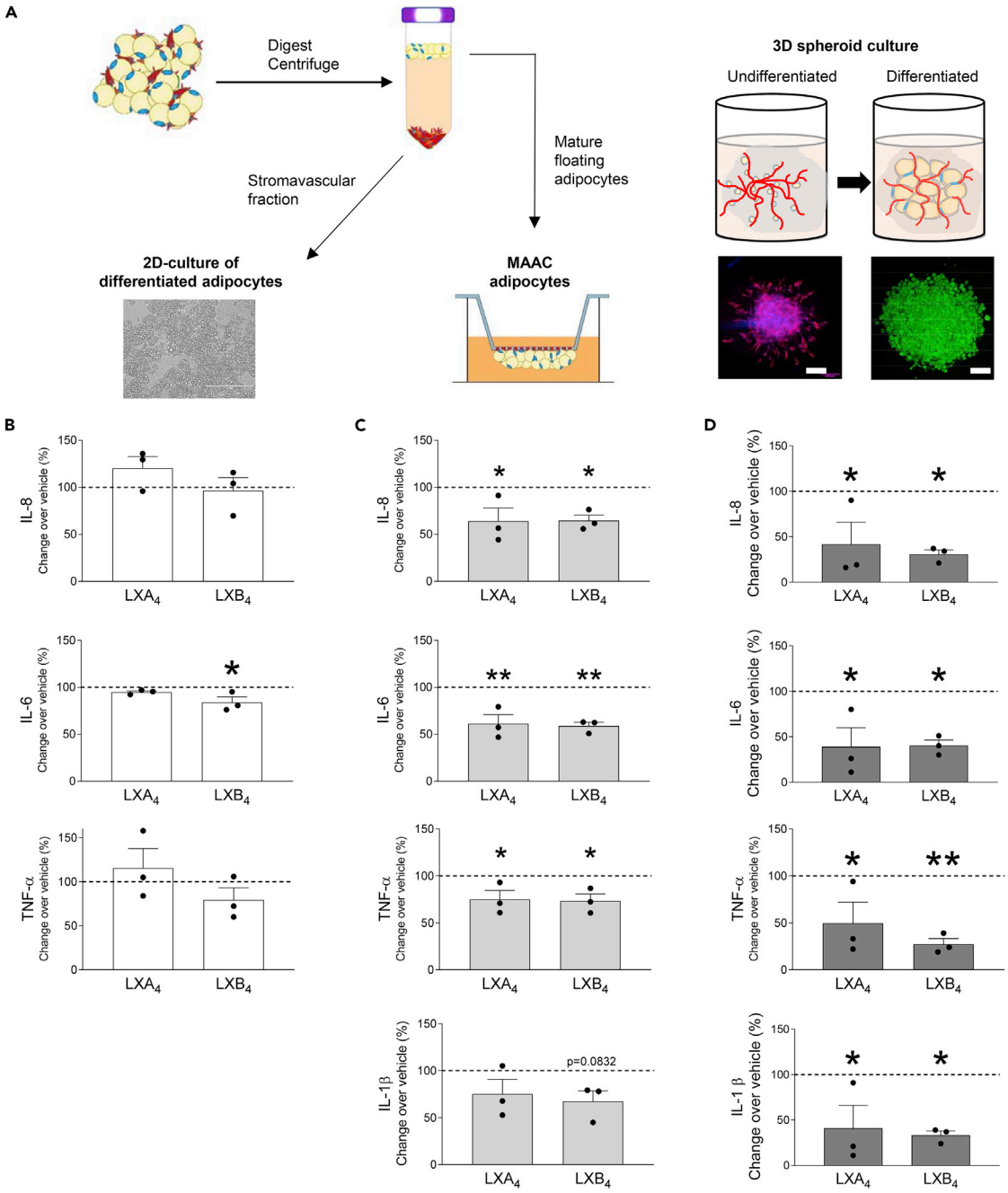

Figure 1. Lipoxins require a 3D environment to robustly attenuate inflammation

(A) Schematic illustration of the 2D- and 3D cell culture models. Scale bar = 200 μm.

(B–D) Levels of pro-inflammatory cytokines in the supernatant of human 2D-cultured adipocytes (B), MAAC 3D cultures (C), and 3D spheroids (D) treated with vehicle, LXA_4, or LXB_4. Controls are set to 100% (dashed line). Statistical analysis was determined using ANOVA with the least significant difference post-hoc comparison test. Data are presented as mean ± SEM. *p < 0.05, **p < 0.01. n = 3.

switch toward a pro-resolving M2 macrophage phenotype. No difference in M1 macrophage *ITGAX* (coding for CD11c) expression was observed in either of the patient subgroups (Figure 2D). These findings were corroborated in stained sections of lipoxin-treated adipose tissue explants, showing unaltered numbers of $CD68^+CD11c^+$ M1 macrophages, while amounts of $CD68^+CD206^+$ M2 macrophages increased, albeit only in responders treated with LXB_4 (Figures 2E and 2F). The relatively brief incubation time of 6 h during *ex vivo* cultures may account for the observed difference between treated human adipose tissues and our previous

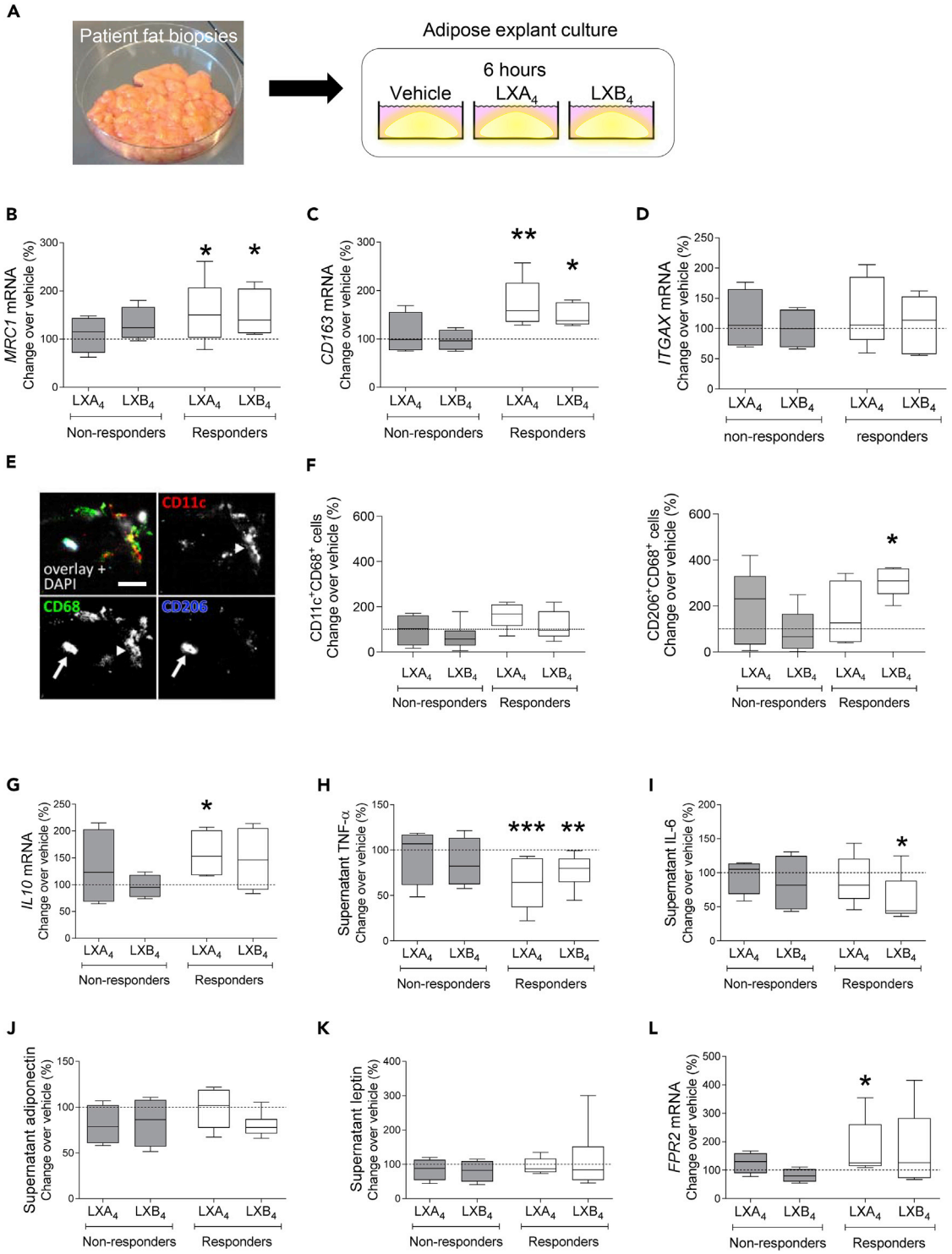

Figure 2. Lipoxins reduce obesity-related inflammation in human adipose tissue explants from patients with elevated CRP levels

(A) Schematic illustration of the experimental approach, where adipose tissue explants from patients were treated with vehicle, LXA_4, or LXB_4 for 6 h, after which the tissue mRNA and supernatant cytokine levels were analyzed and immunohistochemistry was performed.

(B–F) Macrophage markers were quantified by mRNA expression (B–D: M2 markers *MRC1*, *CD163*, and M1 marker *ITGAX*) and immunofluorescence co-localization (E–F: CD68 pan-marker, CD11c M1 marker, and CD206 M2 marker). (E) CD68: green in overlay, CD11c: red in overlay, CD206: blue in overlay, DAPI: white in overlay. Arrow highlights $CD206^+$,$CD68^+$ (M2) macrophages, arrowhead highlights $CD11c^+$,$CD68^+$ (M1) macrophages. Scalebar = 20μm.

Figure 2. *Continued*

(G–K) Cytokine and adipokine expression. G: Interleukin (*IL*)-*10* mRNA, H-K: Supernatant levels of TNF-α, IL-6, adiponectin and leptin.

(L) mRNA expression of the LXA_4 receptor *FPR2*. Dashed line represents the patients' individual baseline expression set to 100%, in non-responder and responder groups, respectively. Statistical analysis was done by Kruskal-Wallis test with Dunn's post-hoc comparison. Data are presented as mean ± SEM. *p < 0.05, **p < 0.01, ***p < 0.001. Figure relates to Figures S1 and S3.

studies in mice (Börgeson et al., 2015). Lipoxins did not affect adipose tissue expression of T cell markers CD4, CD8, and CD69 (Figure S1A). We also quantified cytokine and adipokine levels to characterize the donor's functional response. In the responder cohort, LXA_4 treatment increased expression of the anti-inflammatory cytokine *IL-10 mRNA* (Figure 2G). Lipoxin treatment decreased levels of pro-inflammatory TNF-α and IL-6, although the latter was only seen with LXB_4 (Figures 2H and 2I). LXA_4-mediated protection against obesity-related pathophysiology is independent of adiponectin in mice (Börgeson et al., 2015). This finding is consistent in humans, as neither lipoxin altered levels of adiponectin or leptin (Figures 2J and 2K).

We tested if differences between the patient subgroups were related to altered SPM receptor expression, focusing on the LXA_4 receptor FPR2/ALX (Perretti and Godson, 2020). Baseline expression of FPR2/ALX in adipose tissues collected during surgery did not differ significantly between responders and non-responders. However, LXA_4 treatment significantly increased FPR2/ALX levels in explants of responders only (Figure 2L). No significant effect on FPR2/ALX levels was seen with LXB_4. FPR2/ALX localization was also unaltered (Figure S1B).

Importantly, baseline levels of all investigated marker proteins in vehicle-treated adipose tissue explants were similar between responders and non-responders (Figure S3). Only the response to lipoxin treatment differentiated the groups.

Lipoxin responders are characterized by altered inflammatory and adipose tissue lipid profiles

CRP originates from the liver and other cells, including adipocytes (Chen et al., 2020). However, elevated CRP levels in responders were primarily derived from the liver, as CRP expression was low in omental white adipose tissue (Figure 3A). Patient plasma CRP levels correlated with their responsiveness to lipoxin treatment, as determined by altered CD206 gene expression in lipoxin-treated adipose tissue explants (Figure 3B). Importantly, responders and non-responders displayed comparable levels of traditional markers of systemic inflammation as evidenced by multiplex screening of inflammatory plasma proteins, despite the altered CRP levels (Figure 3C and Table S1).

Next, we wondered whether there are transcriptional differences between adipose tissues of responders versus non-responders. Analysis of sex-matched transcriptomes using RNA-Seq between these two groups resulted in 11 significantly differentially expressed genes with a $\log_2$ fold change of at least 0.5 (Figure 3D). The list includes several genes associated with altered inflammatory state or metabolic syndrome, such as an interleukin-2 receptor subunit (*IL2RA*) or casein alpha s1 (*CSN1S1*).

We hypothesized that elevated CRP levels in responders may trigger inflammation in adipose tissues. Indeed, treating human adipocytes with 10 ng/mL CRP increased levels of pro-inflammatory cytokines IL-1β, IL-8, and IL-6, while not affecting adiponectin (Figure 3E).

We also performed a targeted oxylipin screen on fat biopsies to gain insights into the lipidome environment of responders vs. non-responders. Responders had elevated levels of adipose tissue thromboxane B2 (TXB2), 12(13)-EpODE, and prostaglandin D2 (PGD2), while showing reduced levels of 9(10)- and 15(16)-DiHODE or the related 9(10)-DiHOME (Figure 3F). We also found reduced diol/epoxide ratios in responders, which support decreased turnover and activity of soluble epoxide hydrolase (sEH) (Figures 3G and 3H). Responders were also characterized by higher PGD2 (Figure 3F).

DISCUSSION

Adipose tissue inflammation is a known driver of obesity-related cardiometabolic diseases (Börgeson and Sharma, 2013; Henning, 2021). Administration of specialized lipid mediators, such as the lipoxins, which resolve inflammation and alleviate associated cardiometabolic diseases have thus been proposed as a

Table 1. Cohort characteristics and clinical parameters.

Category	Variable	Controls	Non-responders	Responders	Controls vs non-responders p value	Controls vs responders p value	Non-responders vs responders p value
Cohort characteristics	Sex	12 ♀/3 ♂	5 ♀/2 ♂	7 ♀/1 ♂	N/A	N/A	N/A
	Age, years	41.0 (32.0–51.0)	47.0 (32.0–48.5)	40.5 (30.8–55.0)	0.828	0.925	0.911
	Caucasian/White ethnicity	15/15	7/7	8/8	N/A	N/A	N/A
Adiposity	BMI, kg/m^2	22.7 (21.1–23.5)	39.9 (38.2–40.8)	40.1 (38.3–41.7)	**p < 0.001**	**p < 0.001**	0.814
	Weight, kg	63.0 (58.6–65.1)	130.0 (123.4–130.4)	116.6 (99.3–122.7)	**p < 0.001**	**0.001**	0.347
	Sagittal height, cm	17.5 (16.0–18.8)	26.5 (25.8–28.2)	27.2 (26.0–28.0)	**p < 0.001**	**p < 0.001**	0.976
	Waist circumference, cm	77.0 (73.2–87.5)	122.0 (111.0–129.2)	116.5 (110.2–125.1)	**p < 0.001**	**p < 0.001**	0.906
	Waist-to-height ratio, %	47.6 (44.0–50.1)	66.7 (64.5–72.0)	70.9 (65.9–74.1)	**0.001**	**p < 0.001**	0.597
	Fasting glucose, mmol/L	5.5 (5.0–6.1)	6.4 (6.2–6.4)	6.1 (5.7–6.7)	**0.013**	0.065	0.522
Inflammation	White blood cells, x10^9/L	4.9 (4.5–5.5)	4.9 (4.3–5.4)	5.8 (4.6–6.9)	0.804	0.230	0.217
	C-reactive protein, mg/L	1.0*(1.0–1.0)	3.0 (1.0–3.5)	7.0 (6.0–12.2)	0.175	**p < 0.001**	**0.006**
Liver function	ALT, μkat/L	0.3 (0.3–0.3)	0.8 (0.6–0.9)	1.0 (0.9–1.8)	**0.007**	**p < 0.001**	0.204
	AST, μkat/L	0.3 (0.3–0.4)	0.5 (0.4–0.5)	0.8 (0.7–1.0)	0.052	**p < 0.001**	0.082
	ALP, μkat/L	0.8 (0.7–1.1)	1.2 (1.0–1.5)	1.3 (1.0–1.6)	0.051	**0.048**	0.956
Hypertension	Diastolic blood pressure, mmHg	74.0 (67.5–82.0)	80.0 (80.0–83.0)	77.0 (71.5–82.0)	0.118	0.558	0.375
	Systolic blood pressure, mmHg	119.0 (114.0–129.0)	128.0 (120.0–136.5)	125.0 (118.5–139.2)	0.194	0.263	0.840
	Heart rate, beats/min	68.0 (64.0–71.5)	79.0 (69.0–82.5)	72.0 (66.0–100.2)	0.122	0.131	0.930
Hyperlipidemia	Cholesterol, mmol/L	4.5 (3.8–6.0)	3.5 (3.2–3.8)	3.5 (2.9–3.7)	0.020	0.012	0.936
	Triglycerides, mmol/L	0.7 (0.6–1.0)	1.1 (1.0–1.1)	0.9 (0.8–1.1)	**0.049**	0.159	0.580
	HDL cholesterol, mmol/L	1.9 (1.6–2.0)	0.9 (0.9–1.0)	1.1 (0.9–1.2)	**p < 0.001**	**0.001**	0.762
	LDL cholesterol, mmol/L	2.8 (2.0–3.7)	2.2 (2.0–2.6)	1.8 (1.7–2.1)	0.301	**0.033**	0.372
Medications	Hypertension medication, n	0/15	2/7	3/8	0.091	0.032	>0.999
	Diabetes medication, n	0/15	0/7	2/8	>0.999	0.111	0.467
	Lipid lowering medication, n	0/15	1/7	1/8	0.318	0.348	>0.999

Data are presented as the median and interquartile range (25–75%). * Asterisk indicates that levels of C-reactive protein in healthy control individuals fall below the limit of detection and are reported as 1.0 mg/L. p values for continuous variables were calculated using Kruskal-Wallis test with Dunn's post-hoc comparisons. p values for categorical variables were calculated using Fishers's exact test. Abbreviations: BMI, Body mass index; ALT, Alanine aminotransferase; AST, Aspartate transaminase; ALP, Alkaline Phosphatase; HDL, High-density lipoprotein; LDL, Low-density lipoprotein.

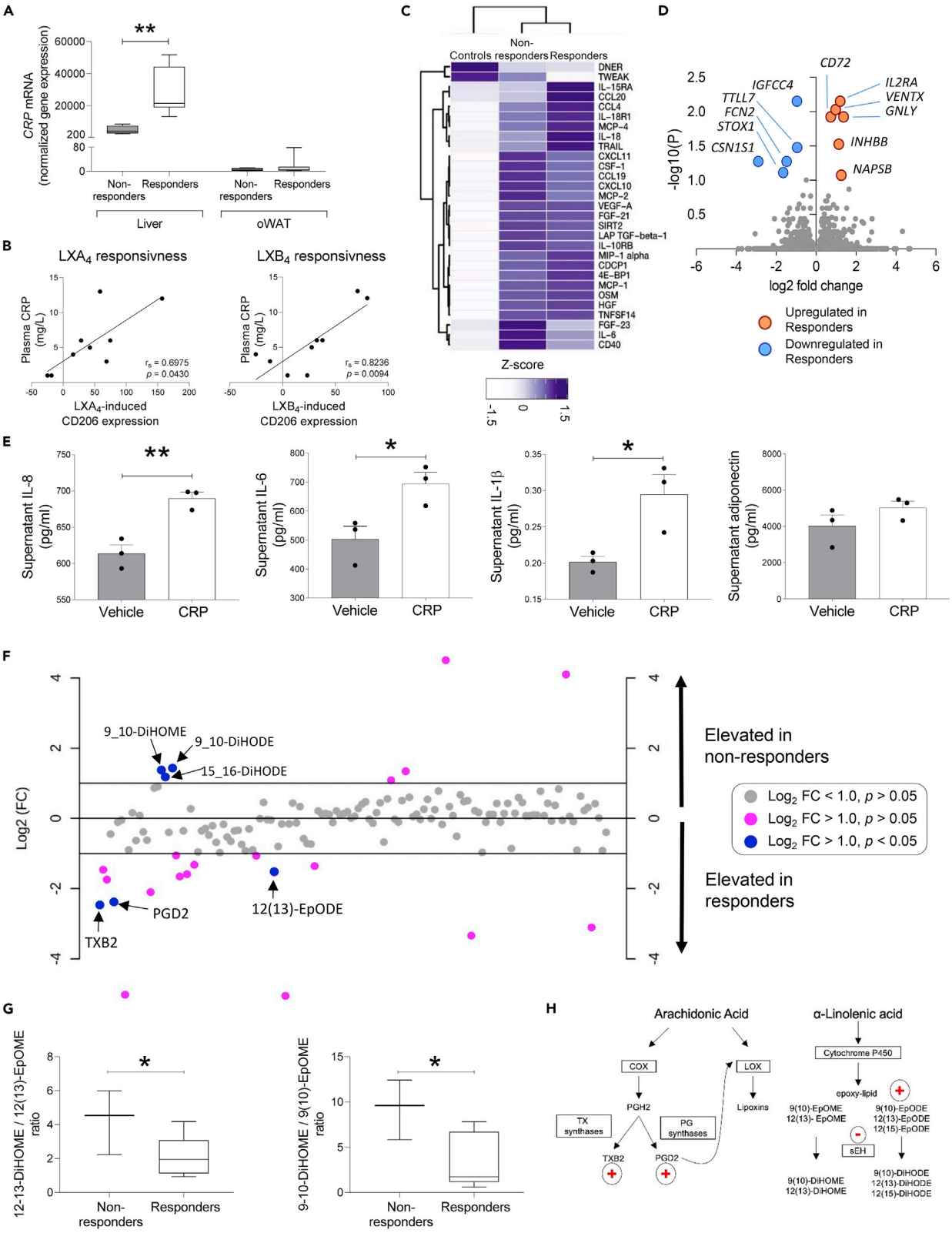
A
CRP mRNA (normalized gene expression)
Non-responders
Responders
Liver
oWAT
B
LXA4 responsivness
LXB4 responsivness
Plasma CRP (mg/L)
LXA4-induced CD206 expression
LXB4-induced CD206 expression
C
Controls
Non-responders
Responders
Z-score
D
log2 fold change
-log10(P)
Upregulated in Responders
Downregulated in Responders
E
Supernatant IL-8 (pg/ml)
Supernatant IL-6 (pg/ml)
Supernatant IL-1β (pg/ml)
Supernatant adiponectin (pg/ml)
Vehicle
CRP
F
Log2 (FC)
9_10-DiHOME
9_10-DiHODE
15_16-DiHODE
PGD2
TXB2
12(13)-EpODE
Elevated in non-responders
Elevated in responders
G
12-13-DiHOME / 12(13)-EpOME ratio
9-10-DiHOME / 9(10)-EpOME ratio
H
Arachidonic Acid
α-Linolenic acid
COX
LOX
PGH2
TX synthases
PG synthases
Lipoxins
Cytochrome P450
epoxy-lipid
sEH

Figure 3. Lipoxin responders are characterized by altered inflammatory and adipose tissue lipid profiles

(A) *CRP* mRNA levels in liver (left panel) and omental white adipose tissue (oWAT) (right panel) in responders and non-responders.

(B) Spearman's correlation between patients' plasma CRP levels and responsiveness to lipoxin treatment, determined as altered *CD206* gene expression in lipoxin-treated adipose tissue explants.

(C) Hierarchical clustering of significantly altered inflammatory plasma markers identified via Olink multiplexed protein arrays in healthy individuals, responders, and non-responders.

(D) Transcriptome comparison of mRNAs in omental white adipose tissues from responders versus non-responders. Highlighted are significantly differentially expressed genes that were downregulated (blue) or upregulated in female patients of the responder group compared with non-responder group. Data are shown as $\log_2$ fold change in gene expression, vs $-\log_{10}$ FDR adjusted p values. (E) Levels of secreted pro-inflammatory cytokines and adiponectin in adipocyte cultures treated with vehicle or CRP (10 ng/mL).

(F) Targeted lipidomics of omental adipose tissue to assess oxylipin levels. Lipids shown in blue retained statistical significance besides having a $\log_2$ fold change value greater than one, whereas lipids represented in pink did not retain statistical significance.

(G) Diol/epoxide ratios as a measure of soluble epoxy hydrolase (sEH) activity.

(H) Schematic outline of relevant lipid pathways and characteristic changes in responders (in red). Statistical analysis was determined by Mann-Whitney U test and p values from transcriptome differential gene expression analysis were FDR corrected for multiple comparisons. Data are presented as mean ± SEM. *$p < 0.05$, **$p < 0.01$. Figure relates to Table S1.

therapeutic approach. Here, we investigated how lipoxins affect human adipocytes grown in culture and in patient-specific adipose tissue explants.

We first tested the effects of prolonged lipoxin treatment using three culture models of differentiated primary human adipocytes *in vitro*. It is debated which method is most suitable for the culture of adipocytes (Ravi et al., 2015). 2D cultures of differentiated adipocytes are widely adopted, although these cells differ from mature adipocytes *in vivo*, being smaller in size and lacking a unilocular lipid droplet. This has led to the development of other culture methods, such as the MAAC (Harms et al., 2019) or the HUVAS (Ioannidou et al., 2021) models. These 3D culture systems allow isolated adipocytes to either maintain or form a large unilocular lipid droplet in a physiological manner. Our data show that LXA_4 and LXB_4 significantly reduce inflammation in 3D-cultured MAAC and spheroid systems, while 2D-cultured adipocytes showed little responsiveness to the SPMs in our hands. The discrepancy between models may be reflective of biological deficiencies in the 2D cell culture, where important aspects of the adipocyte morphology and differentiation cues are missing. Indeed, the 2D adipocyte model requires additional growth factors to drive differentiation, which may result in a variability in differentiation efficiency and cell maturity. Thus, 2D-cultured adipocytes are smaller in size and lack a unilocular lipid droplet as compared to the 3D-cultured cells (Alexandersson et al., 2020; Harms et al., 2019). These differences may significantly affect the cell's biology, rendering 2D-cultured adipocytes less responsive to SPM treatment. Summarized, our data imply the critical need to use 3D culture methods when investigating the lipoxin-mediated bioactions and working with human adipocytes *in vitro*.

We also tested if lipoxin treatment could reduce obesity-related inflammation in adipose tissue explants obtained from gastric bypass patients. This 3D culture system mimics a physiological environment of intact adipose tissue as it retains the intact extracellular matrix and includes all resident cell types, such as endothelial cells or leukocytes. In addition, explant cultures allow for investigation of patient-specific drug effects. Using these adipose tissue explant cultures, our study establishes the first proof-of-concept evidence that lipoxins might be used to attenuate obesity-induced inflammation in human subjects with low-grade systemic inflammation. However, our data also suggest that lipoxin treatment in humans may require a tailored personalized-medicine approach to be effective, as only a subgroup of patients characterized by high CRP levels responded to the drug.

Elevated CRP levels are proposed to reflect a state of chronic low-grade inflammation in obese individuals, correlating with BMI and metabolic syndrome (Ellulu et al., 2017). Multiple prospective studies use CRP to predict incidence of myocardial infarction, stroke, peripheral vascular disease, and sudden cardiac death (Ridker et al., 2003). While CRP has been shown to induce inflammation in mouse cells (Yuan et al., 2007), it was to our knowledge previously unknown how human adipocytes react to the acute phase protein. Our data suggest that CRP affects adipocytes directly, resulting in the production of pro-inflammatory cytokines. Thus, elevated CRP levels observed in responders may trigger inflammation in the patient's adipose tissue, potentially "priming" the tissue to be more responsive to SPM treatment.

CRP is one of the most commonly used markers of systemic inflammation in the clinic. We also investigated if additional clinical parameters used to assess inflammation and metabolic health could further

differentiate our cohorts, in addition to CRP. However, no significant difference in total white blood cell counts, plasma cytokines, hypertension, hyperlipidemia, or diabetes between non-responders and responders were found (Table 1). Our analyses also indicate that individuals in both groups defy the separation into metabolically "healthy" or "unhealthy" phenotypes. Thus, only the chronic low-grade elevation of plasma CRP levels was a specific characteristic of the lipoxin responder group.

We also performed RNA-Seq and oxylipin analyses, to gain unbiased insight into transcriptional changes or the lipidome environment of adipose tissues from responders and non-responders, respectively. While the overall number of differentially expressed genes identified in our RNA-Seq analysis between the two groups was surprisingly low, we identified several genes associated with altered inflammatory state or metabolic syndrome. Specifically, responders downregulated immunoglobulin superfamily DCC subclass member 4 [*IGDCC4*], which has been shown to play roles during endocytosis of viral particles (Song et al., 2021), or casein alpha s1 [*CSN1S1*]), an adipose tissue-specific gene involved in immune and inflammatory responses that is found upregulated in adipose tissues of obese individuals (Nono Nankam et al., 2020). Conversely, responders upregulated interleukin-2 receptor subunit alpha [*IL2RA*] mRNA encoding for IL-2Rα (CD25), a protein that forms part of the trimeric interleukin-2 (IL2) receptor complex. The IL-2Rα subunit can also be proteolytically cleaved by metalloproteinases to form a soluble peptide (sIL-2Rα) which is released into the extracellular space (Sheu et al., 2001). *IL2RA* has been proposed as a biomarker for systemic inflammation, and signaling linked to interleukin-2 and its receptor was shown to play important roles in regulating immunity and immune tolerance (Buhelt et al., 2021; Durda et al., 2015). Besides *IL2RA*, responders also had elevated expression of granulysin [*GNLY*], a cytotoxic protein secreted from T lymphocytes or natural killer cells. Intriguingly, both IL-2Rα and granulysin were either shown or hypothesized to correlate with elevated circulating CRP levels in cardiovascular disease (Buhelt et al., 2021; Durda et al., 2015; Persic et al., 2018). Our oxylipin screen also revealed several differences between adipose tissues from responders and non-responders. Specifically, both groups showed distinct changes to levels of TXB2, prostaglandin D2, and several alpha-linolenic acid (ALA) metabolites. TXB2 is a marker of platelet activation that is elevated in mild, but not in morbid obesity (Graziani et al., 2011). Prostaglandins have dual roles in regulating inflammatory responses and induce the expression of lipoxygenase (LOX) required for SPM production (Levy et al., 2001). Although weight loss can reverse obesity-induced changes to the lipidome, adipose tissue retains a persistent obese signature characterized by sustained elevation of prostaglandins and downstream metabolites (Hernandez-Carretero et al., 2018). Elevated PGD2 levels in responders may therefore represent another factor "priming" this cohort to be receptive to SPM treatment. We also noted characteristic differences in alpha-linolenic acid (ALA) metabolites. Responders had elevated levels of the epoxy-lipid 12(13)-EpODE, which is produced by inflammatory leukocytes (Thompson and Hammock, 2007), but has also been associated with anti-inflammatory actions (Imig and Hammock, 2009). Conversely, downstream epoxy-lipid metabolites, such as 9(10)- and 15(16)-DiHODE or the related 9(10)-DiHOME, were reduced. Alterations to diol/epoxide ratios in responders suggested a changed activity of soluble epoxide hydrolase (sEH). Soluble EH is elevated in the adipose tissue of obese rodents (De Taeye et al., 2010) and interlinked with cardiometabolic disease. Inhibitors of sEH act as anti-inflammatory agents, and may stimulate the production of LXA_4 (Imig and Hammock, 2009; Ono et al., 2014).

In conclusion, our study raises important considerations when designing investigations into therapeutic effects of pro-resolving mediators, such as lipoxins, in human obesity and cardiometabolic disease. Lipoxins reduced inflammation in adipose tissue explants of a subpopulation of patients that were characterized by high CRP levels. Indeed, the amplitude of the lipoxin-mediated response in all patients was correlated with their plasma CRP levels. In lipoxin responder patients, the drug increased expression of anti-inflammatory and pro-resolving markers, while reducing pro-inflammatory cytokines, and these effects were independent of adipokine secretion. Importantly, responders also upregulated LXA_4 receptor levels in response to lipoxin treatment. Future studies are required to further delineate the exact mechanisms and inter-organ crosstalk involved in the patient-specific effects of lipoxin treatment.

Limitations of the study

A limitation of this study is that the clinical sample size was relatively small, making it difficult to draw any conclusions regarding the impact of sex. However, as each patient is compared to their individual baseline, the drug-induced effects remain valid. Further studies may clarify some of the pharmacological and cellular mechanisms involved in the lipoxin-mediated effects in non-responder versus responder patients. We separated the responders and non-responders based on their endogenous CRP levels, as this appeared

to be the most predominant clinical characteristic that correlated with lipoxin efficacy. However, future studies should evaluate this finding in a larger cohort.

It should also be noted that the adipose tissue used in the 3D cell culture models were derived from subcutaneous fat, whereas the adipose tissue explants were obtained from the omental fat region. These types of adipose tissue have significant biological differences (Soták et al., 2022) and data should be interpreted considering these limitations.

Another significant limitation of this study is that all participants in this Swedish study were of Caucasian/White origin. This is important to consider when designing future trials. Hence, our data should be interpreted with caution when relating the findings to different ethnicities.

STAR★METHODS

Detailed methods are provided in the online version of this paper and include the following:

- KEY RESOURCES TABLE
- RESOURCE AVAILABILITY
  - Lead contact
  - Materials availability
  - Data and code availability
- EXPERIMENTAL MODEL AND SUBJECT DETAILS
  - Study design and human subjects
  - Categorizing responders vs. non-responders
- METHOD DETAILS
  - Clinical blood analyses
  - Plasma protein screen
  - Adipose tissue explant culture
  - Immunofluorescence
  - Cell isolation from human adipose tissue
  - Membrane mature adipocyte aggregate culture (MAAC) model
  - Differentiated human adipocyte culture
  - Human unilocular vascularized adipocyte spheroid (HUVAS) cultures
  - Gene expression analyses
  - Targeted lipidomics analyses
- QUANTIFICATION AND STATISTICAL ANALYSIS
- ADDITIONAL RESOURCES

SUPPLEMENTAL INFORMATION

Supplemental information can be found online at https://doi.org/10.1016/j.isci.2022.104602.

ACKNOWLEDGMENTS

We thank Catherine Åhlund for help collecting material. EB is supported by WCMTM, the Knut and Alice Wallenberg Foundation, the Swedish Research Council (#2016/82), SSMF (#S150086), and an ERC StG (#804418). The NIH West Coast Metabolomics Center is funded through the NIH (U24 DK097154, NIH U2C 030158, NIH U24 DK097154 (OF)) with additional support by USDA (#2032-51530-022-00D, #2032-51530-025-00D (JWN)). SL is supported by grants from the NIH (HL128457, HL107744), the Swedish Heart-Lung Foundation (#20180199) and the Novo Nordisk Foundation (NNF20OC0062812). CEH is supported by the Swedish Research Council (#2019-02046), Jeanssons Stiftelse (#2020-0010), Åke Wibergs Stiftelse (M20-022), Tore Nilssons Stiftelse (2020-00853), and Karolinska Institutet. Sequencing was performed by the SNP&SEQ Technology Platform in Uppsala. The facility is part of the National Genomics Infrastructure (NGI) Sweden and Science for Life Laboratory. The SNP&SEQ Platform is also supported by the Swedish Research Council and the Knut and Alice Wallenberg Foundation.

AUTHOR CONTRIBUTIONS

EB and VW conceived and designed the project. MS, MRR, MC, AR, JDK, DT, CB, PA, TS, and VW collected samples. MS, MRR, MC, AR, JDK, DT, TS, KB, CEH, and EB performed experiments. MS, MRR, MC, MH, OF,

JWN, MQJ, JB, SL, and EB analyzed and interpreted the data. VW and TS recruited patients. EB wrote the paper. All authors commented on the manuscript.

DECLARATION OF INTERESTS

The authors declare no competing interests.

Received: December 30, 2021
Revised: March 16, 2022
Accepted: June 8, 2022
Published: July 15, 2022

REFERENCES

Agrawal, K., Hassoun, L.A., Foolad, N., Borkowski, K., Pedersen, T.L., Sivamani, R.K., and Newman, J.W. (2018). Effects of atopic dermatitis and gender on sebum lipid mediator and fatty acid profiles. Prostaglandins Leukot. Essent. Fatty Acids *134*, 7–16. https://doi.org/10.1016/j.plefa.2018.05.001.

Alexandersson, I., Harms, M.J., and Boucher, J. (2020). Isolation and culture of human mature adipocytes using membrane mature adipocyte aggregate cultures (MAAC). JoVE *10*. https://doi.org/10.3791/60485.

Bielawski, J., Szulc, Z.M., Hannun, Y.A., and Bielawska, A. (2006). Simultaneous quantitative analysis of bioactive sphingolipids by high-performance liquid chromatography-tandem mass spectrometry. Methods *39*, 82–91. https://doi.org/10.1016/j.ymeth.2006.05.004.

Börgeson, E., Johnson, A.M., Lee, Y.S., Till, A., Syed, G.H., Ali-Shah, S.T., Guiry, P.J., Dalli, J., Colas, R.A., Serhan, C.N., et al. (2015). Lipoxin A4 attenuates obesity-induced adipose inflammation and associated liver and kidney disease. Cell Metabol. *22*, 125–137. https://doi.org/10.1016/j.cmet.2015.05.003.

Börgeson, E., McGillicuddy, F.C., Harford, K.A., Corrigan, N., Higgins, D.F., Maderna, P., Roche, H.M., and Godson, C. (2012). Lipoxin A4 attenuates adipose inflammation. FASEB. J. *26*, 4287–4294. https://doi.org/10.1096/fj.12-208249.

Börgeson, E., and Sharma, K. (2013). Obesity, immunomodulation and chronic kidney disease. Curr. Opin. Pharmacol. *13*, 618–624. https://doi.org/10.1016/j.coph.2013.05.011.

Buhelt, S., Søndergaard, H.B., Mahler, M.R., Cobanovic, S., Börnsen, L., Ammitzbøll, C., Oturai, A.B., and Sellebjerg, F. (2021). Biomarkers of systemic inflammation, soluble IL-2Rα and the multiple sclerosis-associated IL2RA SNP rs2104286 in healthy subjects and multiple sclerosis patients. Mult. Scler. Relat. Disord. *54*, 103140. https://doi.org/10.1016/j.msard.2021.103140.

Chen, J.-Y., Zhu, X.-L., Liu, W.-H., Xie, Y., Zhang, H.-F., Wang, X., Ying, R., Chen, Z.-T., Wu, M.-X., Qiu, Q., et al. (2020). C-reactive protein derived from perivascular adipose tissue accelerates injury-induced neointimal hyperplasia. J. Transl. Med. *18*, 68. https://doi.org/10.1186/s12967-020-02226-x.

Clària, J., Nguyen, B.T., Madenci, A.L., Ozaki, C.K., and Serhan, C.N. (2013). Diversity of lipid mediators in human adipose tissue depots. Am. J. Physiol. Cell Physiol. *304*, C1141–C1149. https://doi.org/10.1152/ajpcell.00351.2012.

De Taeye, B.M., Morisseau, C., Coyle, J., Covington, J.W., Luria, A., Yang, J., Murphy, S.B., Friedman, D.B., Hammock, B.B., and Vaughan, D.E. (2010). Expression and regulation of soluble epoxide hydrolase in adipose tissue. Obesity *18*, 489–498. https://doi.org/10.1038/oby.2009.227.

Dobin, A., Davis, C.A., Schlesinger, F., Drenkow, J., Zaleski, C., Jha, S., Batut, P., Chaisson, M., and Gingeras, T.R. (2012). STAR: ultrafast universal RNA-seq aligner. Bioinformatics *29*, 15–21. https://doi.org/10.1093/bioinformatics/bts635.

Donath, M.Y., Dalmas, É., Dalmas, E., Sauter, N.S., Böni-Schnetzler, M., and Boni-Schnetzler, M. (2013). Inflammation in obesity and diabetes: islet dysfunction and therapeutic opportunity. Cell Metabol. *17*, 860–872. https://doi.org/10.1016/j.cmet.2013.05.001.

Durda, P., Sabourin, J., Lange, E.M., Nalls, M.A., Mychaleckyj, J.C., Jenny, N.S., Li, J., Walston, J., Harris, T.B., Psaty, B.M., et al. (2015). Plasma levels of soluble interleukin-2 receptor α: associations with clinical cardiovascular events and genome-wide association scan. Arterioscler. Thromb. Vasc. Biol. *35*, 2246–2253. https://doi.org/10.1161/atvbaha.115.305289.

Ellulu, M.S., Patimah, I., Khaza'ai, H., Rahmat, A., and Abed, Y. (2017). Obesity and inflammation: the linking mechanism and the complications. Arch. Med. Sci. *4*, 851–863. https://doi.org/10.5114/aoms.2016.58928.

Ewels, P., Magnusson, M., Lundin, S., and Käller, M. (2016). MultiQC: summarize analysis results for multiple tools and samples in a single report. Bioinformatics *32*, 3047–3048. https://doi.org/10.1093/bioinformatics/btw354.

Gabrielsson, B.G., Olofsson, L.E., Sjögren, A., Jernås, M., Elander, A., Lönn, M., Rudemo, M., and Carlsson, L.M.S. (2005). Evaluation of reference genes for studies of gene expression in human adipose tissue. Obes. Res. *13*, 649–652. https://doi.org/10.1038/oby.2005.72.

Godson, C., Mitchell, S., Harvey, K., Petasis, N.A., Hogg, N., and Brady, H.R. (2000). Cutting edge: lipoxins rapidly stimulate nonphlogistic phagocytosis of apoptotic neutrophils by monocyte-derived macrophages. J. Immunol. *164*, 1663–1667. https://doi.org/10.4049/jimmunol.164.4.1663.

Graziani, F., Biasucci, L.M., Cialdella, P., Liuzzo, G., Giubilato, S., Della Bona, R., Pulcinelli, F.M., Iaconelli, A., Mingrone, G., and Crea, F. (2011). Thromboxane production in morbidly obese subjects. Am. J. Cardiol. *107*, 1656–1661. https://doi.org/10.1016/j.amjcard.2011.01.053.

Harms, M.J., Li, Q., Lee, S., Zhang, C., Kull, B., Hallen, S., Thorell, A., Alexandersson, I., Hagberg, C.E., Peng, X.R., et al. (2019). Mature human white adipocytes cultured under membranes maintain identity, function, and can Transdifferentiate into Brown-like adipocytes. Cell Rep. *27*, 213–225.e5. https://doi.org/10.1016/j.celrep.2019.03.026.

Henning, R.J. (2021). Obesity and obesity-induced inflammatory disease contribute to atherosclerosis: a review of the pathophysiology and treatment of obesity. Am. J. Cardiovasc. Dis. *11*, 504–529.

Hernandez-Carretero, A., Weber, N., La Frano, M.R., Ying, W., Lantero Rodriguez, J., Sears, D.D., Wallenius, V., Wallenius, V., Borgeson, E., Newman, J.W., et al. (2018). Obesity-induced changes in lipid mediators persist after weight loss. Int. J. Obes. *42*, 728–736. https://doi.org/10.1038/ijo.2017.266.

Imig, J.D., and Hammock, B.D. (2009). Soluble epoxide hydrolase as a therapeutic target for cardiovascular diseases. Nat. Rev. Drug Discov. *8*, 794–805. https://doi.org/10.1038/nrd2875.

Ioannidou, A., Alatar, S., Schipper, R., Baganha, F., Ahlander, M., Hornell, A., Fisher, R.M., and Hagberg, C.E. (2021). Hypertrophied human adipocyte spheroids as in vitro model of weight gain and adipose tissue dysfunction. J. Physiol. *600*, 869–883. https://doi.org/10.1113/JP281445.

Kraft, J.D., Blomgran, R., Lundgaard, I., Quiding-Järbrink, M., Bromberg, J.S., and Börgeson, E. (2021). Specialized pro-resolving mediators and the lymphatic system. Int. J. Mol. Sci. *22*, 2750. https://doi.org/10.3390/ijms22052750.

Levy, B.D., Clish, C.B., Schmidt, B., Gronert, K., and Serhan, C.N. (2001). Lipid mediator class switching during acute inflammation: signals in resolution. Nat. Immunol. *2*, 612–619. https://doi.org/10.1038/89759.

Liao, Y., Smyth, G.K., and Shi, W. (2013). featureCounts: an efficient general purpose program for assigning sequence reads to genomic features. Bioinformatics *30*, 923–930. https://doi.org/10.1093/bioinformatics/btt656.

López-Vicario, C., Titos, E., Walker, M.E., Alcaraz-Quiles, J., Casulleras, M., Durán-Güell, M., Flores-Costa, R., Pérez-Romero, N., Forné, M., Dalli, J., and Clària, J. (2019). Leukocytes from obese individuals exhibit an impaired SPM signature. FASEB. J. *33*, 7072–7083. https://doi.org/10.1096/fj.201802587R.

Love, M.I., Huber, W., and Anders, S. (2014). Moderated estimation of fold change and dispersion for RNA-seq data with DESeq2. Genome Biol. *15*, 550. https://doi.org/10.1186/s13059-014-0550-8.

Midtbø, L.K., Borkowska, A.G., Bernhard, A., Rønnevik, A.K., Lock, E.J., Fitzgerald, M.L., Torstensen, B.E., Liaset, B., Brattelid, T., Pedersen, T.L., et al. (2015). Intake of farmed Atlantic salmon fed soybean oil increases hepatic levels of arachidonic acid-derived oxylipins and ceramides in mice. J. Nutr. Biochem. *26*, 585–595. https://doi.org/10.1016/j.jnutbio.2014.12.005.

Nidorf, S.M., Fiolet, A.T.L., Mosterd, A., Eikelboom, J.W., Schut, A., Opstal, T.S.J., The, S.H.K., Xu, X.F., Ireland, M.A., Lenderink, T., et al. (2020). Colchicine in patients with chronic coronary disease. N. Engl. J. Med. *383*, 1838–1847. https://doi.org/10.1056/NEJMoa2021372.

Nono Nankam, P.A., Blüher, M., Kehr, S., Klöting, N., Krohn, K., Adams, K., Stadler, P.F., Mendham, A.E., and Goedecke, J.H. (2020). Distinct abdominal and gluteal adipose tissue transcriptome signatures are altered by exercise training in African women with obesity. Sci. Rep. *10*, 10240. https://doi.org/10.1038/s41598-020-66868-z.

Olefsky, J.M., and Glass, C.K. (2010). Macrophages, inflammation, and insulin resistance. Annu. Rev. Physiol. *72*, 219–246. https://doi.org/10.1146/annurev-physiol-021909-135846.

Ono, E., Dutile, S., Kazani, S., Wechsler, M.E., Yang, J., Hammock, B.D., Douda, D.N., Tabet, Y., Khaddaj-Mallat, R., Sirois, M., et al. (2014). Lipoxin generation is related to soluble epoxide hydrolase activity in severe asthma. Am. J. Respir. Crit. Care Med. *190*, 886–897. https://doi.org/10.1164/rccm.201403-0544OC.

Panigrahy, D., Gilligan, M.M., Serhan, C.N., and Kashfi, K. (2021). Resolution of inflammation: an organizing principle in biology and medicine. Pharmacol. Ther. *227*, 107879. https://doi.org/10.1016/j.pharmthera.2021.107879.

Pedersen, T.L., and Newman, J.W. (2018). Establishing and performing targeted multi-residue analysis for lipid mediators and fatty acids in small clinical plasma samples. Methods Mol. Biol. *1730*, 175–212. https://doi.org/10.1007/978-1-4939-7592-1_13.

Perretti, M., and Godson, C. (2020). Formyl peptide receptor type 2 agonists to kick-start resolution pharmacology. Br. J. Pharmacol. *177*, 4595–4600. https://doi.org/10.1111/bph.15212.

Persic, V., Bastiancic, A.L., Rosovic, I., Raljevic, D., Samsa, D.T., Bastiancic, L., Miskulin, R., Boban, M., and Laskarin, G. (2018). Correlation between immunological-inflammatory markers and endothelial disfunction in the early stage of coronary heart disease. Med. Hypotheses *115*, 72–76. https://doi.org/10.1016/j.mehy.2018.04.001.

Rajan, M.R., Sotak, M., Barrenäs, F., Shen, T., Borkowski, K., Ashton, N.J., Biörserud, C., Lindahl, T.L., Ramström, S., Schöll, M., et al. (2019). Comparative analysis of obesity-related cardiometabolic and renal biomarkers in human plasma and serum. Sci. Rep. *9*, 15385. https://doi.org/10.1038/s41598-019-51673-0.

Ravi, M., Paramesh, V., Kaviya, S.R., Anuradha, E., and Solomon, F.P. (2015). 3D cell culture systems: advantages and applications. J. Cell. Physiol. *230*, 16–26. https://doi.org/10.1002/jcp.24683.

Ridker, P.M., Buring, J.E., Cook, N.R., and Rifai, N. (2003). C-reactive protein, the metabolic syndrome, and risk of incident cardiovascular events: an 8-year follow-up of 14 719 initially healthy American women. Circulation *107*, 391–397. https://doi.org/10.1161/01.cir.0000055014.62083.05.

Ridker, P.M., Everett, B.M., Thuren, T., MacFadyen, J.G., Chang, W.H., Ballantyne, C., Fonseca, F., Nicolau, J., Koenig, W., Anker, S.D., et al. (2017). Antiinflammatory therapy with Canakinumab for atherosclerotic disease. N. Engl. J. Med. *377*, 1119–1131. https://doi.org/10.1056/NEJMoa1707914.

Serhan, C.N., Gupta, S.K., Perretti, M., Godson, C., Brennan, E., Li, Y., Soehnlein, O., Shimizu, T., Werz, O., Chiurchiù, V., et al. (2020). The atlas of inflammation resolution (AIR). Mol. Aspect. Med. *74*, 100894. https://doi.org/10.1016/j.mam.2020.100894.

Serhan, C.N., and Levy, B.D. (2018). Resolvins in inflammation: emergence of the pro-resolving superfamily of mediators. J. Clin. Invest. *128*, 2657–2669. https://doi.org/10.1172/JCI97943.

Sheu, B.C., Hsu, S.M., Ho, H.N., Lien, H.C., Huang, S.C., and Lin, R.H. (2001). A novel role of metalloproteinase in cancer-mediated immunosuppression. Cancer Res. *61*, 237–242.

Song, Y., Huang, H., Hu, Y., Zhang, J., Li, F., Yin, X., Shi, J., Li, Y., Li, C., Zhao, D., and Chen, H. (2021). A genome-wide CRISPR/Cas9 gene knockout screen identifies immunoglobulin superfamily DCC subclass member 4 as a key host factor that promotes influenza virus endocytosis. PLoS Pathog. *17*, e1010141. https://doi.org/10.1371/journal.ppat.1010141.

Soták, M., Casselbrant, A., Rath, E., Zietek, T., Strömstedt, M., Adingupu, D.D., Karlsson, D., Fritsch Fredin, M., Ergang, P., Pácha, J., et al. (2021). Intestinal sodium/glucose cotransporter 3 expression is epithelial and downregulated in obesity. Life Sci. *267*, 118974. https://doi.org/10.1016/j.lfs.2020.118974.

Soták, M., Rajan, M.R., Clark, M., Biörserud, C., Wallenius, V., Hagberg, C.E., and Börgeson, E. (2022). Healthy subcutaneous and omental adipose tissue is associated with high expression of extracellular matrix components. Int. J. Mol. Sci. *23*, 520. https://doi.org/10.3390/ijms23010520.

Stanley, T.L., Zanni, M.V., Johnsen, S., Rasheed, S., Makimura, H., Lee, H., Khor, V.K., Ahima, R.S., and Grinspoon, S.K. (2011). TNF-alpha antagonism with etanercept decreases glucose and increases the proportion of high molecular weight adiponectin in obese subjects with features of the metabolic syndrome. J. Clin. Endocrinol. Metab. *96*, E146–E150. https://doi.org/10.1210/jc.2010-1170.

Tardif, J.C., Kouz, S., Waters, D.D., Bertrand, O.F., Diaz, R., Maggioni, A.P., Pinto, F.J., Ibrahim, R., Gamra, H., Kiwan, G.S., et al. (2019). Efficacy and safety of low-dose colchicine after myocardial infarction. N. Engl. J. Med. *381*, 2497–2505. https://doi.org/10.1056/NEJMoa1912388.

Thompson, D.A., and Hammock, B.D. (2007). Dihydroxyoctadecamonoenoate esters inhibit the neutrophil respiratory burst. J. Biosci. *32*, 279–291. https://doi.org/10.1007/s12038-007-0028-x.

Vandesompele, J., De Preter, K., Pattyn, F., Poppe, B., Van Roy, N., De Paepe, A., and Speleman, F. (2002). Accurate normalization of real-time quantitative RT-PCR data by geometric averaging of multiple internal control genes. Genome Biol. *3*. RESEARCH0034. https://doi.org/10.1186/gb-2002-3-7-research0034.

Yuan, G., Chen, X., Ma, Q., Qiao, J., Li, R., Li, X., Li, S., Tang, J., Zhou, L., Song, H., and Chen, M. (2007). C-reactive protein inhibits adiponectin gene expression and secretion in 3T3-L1 adipocytes. J. Endocrinol. *194*, 275–281. https://doi.org/10.1677/JOE-07-0133.

STAR★METHODS

KEY RESOURCES TABLE

REAGENT or RESOURCE	SOURCE	IDENTIFIER
Antibodies		
FPR2 antibody	Novusbio	NLS1878 lot#A8
Rabbit Anti-CD68 antibody	Abcam	ab213363 lot#GR3266939-1
Mouse Anti-CD11c antibody	Abcam	ab215858 lot#GR3319124-1
Goat Anti-CD206 antibody	R&D	AF2534 lot#VK0115011
Donkey-anti-Rabbit 488	Thermo Fisher	#711-547-003
Donkey-anti-Mouse 594	Thermo Fisher	#715-587-003
Donkey-anti-Goat Cy™5 / 647	Thermo Fisher	#705-175-147
Alexa Fluor 488 Donkey Anti-Rabbit antibody	Jackson Immuno Research	A32814
Biological samples		
Primary human subcutaneous SVF cells	Lonza	PT-5020
Chemicals, peptides, and recombinant proteins		
Qiazol	Qiagen	79306
Trizol	Thermo Fisher	15596018
QIAshredder column	Qiagen	79656
RNeasy Mini Kit	Qiagen	74106
DNAse I	Invitrogen	18068015
Superscript IV Reverse Transcriptase	Invitrogen	18090050
Type 2 collagenase	Worthington	LS004177
K_2EDTA plasma tubes	Greiner Bio One	456279
BSA, fatty acid free	Sigma	A6003
PBS	Corning	21-040-CM
HBSS buffer with Mg^{2+}/Ca^{2+}	Invitrogen	14065149
DMEM	Corning	10-013-CVR
NaCl	Sigma	S5886
KCl	Sigma	529552
KH_2PO_4	Sigma	P5655
$MgSO_4 \cdot 7H_2O$	Sigma	M1880
$CaCl_2 \cdot 2H_2O$	Sigma	C3306
HEPES	Sigma	54457
Penicillin Streptomycin	CellGro (Mediatech)	MT 30-001-CI
Glucose	VWR	101175P
Erythrocyte lysis	Sigma	R7757
Subcutaneous basal media	Ramcon (original manufacturer: ZenBio)	BM-1
bFGF	Sigma	F0291
FBS	Hyclone	SV30160.03
Insulin	Novo Nordisk	Actrapid 5712249103316
Pioglitazone	Sigma	E6910-10MG
IBMX	Sigma	I5879
Dexamethasone	Sigma	D2915

(*Continued on next page*)

Continued

REAGENT or RESOURCE	SOURCE	IDENTIFIER
Citrate unmasking buffer	Cell Signaling	14746
Triton X-100	Sigma	T8787
Tween-20	Sigma	P9416
Glycine	Sigma	G8898
DAPI	Thermo Fisher	D1306
TrueBlack	VWR	23007
Prolong Gold mounting medium	Thermo Fisher	P36930
Endothelial growth medium 2	Lonza	EGM-2, CC-3162
Growth factor-reduced Matrigel	Corning	11553620
Preadipocyte Growth Medium	Lonza	PGM-2, PT-8002
Ethanol absolute ≥99.8%, Molecular biology grade	VWR	437433T
Lipoxin A_4 (LXA_4)	Sigma	#89663-86-5
Lipoxin B_4 (LXB_4)	Cayman	#98049-69-5
Critical commercial assays		
Proseek Multiplex Inflammation I panel	Olink	https://www.olink.com/products/target/inflammation/
Human TNF-α DuoSet ELISA kit	R&D Systems	DY210
Human IL-6 DuoSet ELISA	R&D Systems	DY206
Human IL-8/CXCL8 DuoSet ELISA	R&D Systems	DY208
Human Adiponectin/Acrp30 DuoSet ELISA	R&D Systems	DY1065
Human Leptin DuoSet ELISA	R&D Systems	DY398
Discovery V-PLEX Pro-inflammatory Panel 1 (human)	Meso Scale	K15049D-1
Oligonucleotides		
ddPCR assay *IL10*	Bio-Rad	dHsaCPE5036966
ddPCR assay *MRC1 (CD206)*	Bio-Rad	dHsaCPE5193017
ddPCR assay *CD163*	Bio-Rad	dHsaCPE5050636
ddPCR assay *ITGAX (CD11c)*	Bio-Rad	dHsaCPE5046606
ddPCR assay *FPR2*	Bio-Rad	dHsaCPE5030680
ddPCR assay *CRP*	Bio-Rad	dHsaCPE5036526
ddPCR assay *CD4*	Bio-Rad	dHsaCPE5191723
ddPCR assay *CD69*	Bio-Rad	dHsaCPE5052776
ddPCR assay *CD8a*	Bio-Rad	dHsaCPE5029358
ddPCR assay *CD8b*	Bio-Rad	dHsaCPE5191595
ddPCR assay *LRP10*	Bio-Rad	dHsaCPE5043185
ddPCR assay *RPLP0*	Bio-Rad	dHsaCPE5031575
Software and algorithms		
GraphPad Prism 8	GraphPad Software Inc.	https://www.graphpad.com/
R 4.1.0	The R Project for Statistical Computing	https://www.r-project.org/
R package tidyverse (ver. 1.3.1)	R packages for data science	https://www.tidyverse.org/
CellProfiler 4.2.1	The Broad Institute	https://cellprofiler.org/
Office 365	Microsoft	https://www.office.com/
Fiji	NIH ImageJ	https://imagej.net/software/fiji/
MetaboAnalyst 5.0	Xia Research Group, McGill University	https://www.metaboanalyst.ca/

(*Continued on next page*)

Continued

REAGENT or RESOURCE	SOURCE	IDENTIFIER
Other		
250 μm Polyamid mesh filter	Sintab AB	6111-025043
Separation funnel	VWR	527-0008
Cell factory (10, 5 and 2 layer)	Corning, Costar	3271, 3313, 3269
96-well ultra-low attachment plate	Corning, Costar	CLS7007

RESOURCE AVAILABILITY

Lead contact

Further information and requests for resources and reagents should be directed to and will be fulfilled by the lead contact, Emma Börgeson (emma.borgeson@wlab.gu.se).

Materials availability

This study did not generate new unique reagents.

Data and code availability

- All data reported in this paper will be shared by the lead contact upon request.
- This paper did not generate new original code.
- Any additional information required to reanalyze the data reported in this paper is available from the lead contact upon request.

EXPERIMENTAL MODEL AND SUBJECT DETAILS

Study design and human subjects

Obese subjects aged 18–65 years old were included in this study. Abdominoplasty surgery patients (BMI >30 kg/m^2) donated subcutaneous adipose tissue to prepare cells for the 2D-culture and the MAAC model. We also included gastric bypass surgery patients (BMI >35 with at least one co-morbidity, or BMI>40), who donated adipose tissue either snap-frozen for patient-specific analyses or used for the explant cultures. The latter cohort also donated blood samples and a liver biopsy. Subjects were excluded if they were taking anti-inflammatory and/or immunosuppressive drugs, currently smoked, or were diagnosed with significant gastrointestinal or inflammatory bowel disease. Patients unable to undergo surgery (due to anorexia, allergic reactions and/or other surgical problems) or who had an ongoing infection (e.g., fever or CRP >40 mg/L) were excluded. A control group of lean and metabolically healthy individuals was recruited to provide blood samples and clinical measurements. The control group was age- and sex-matched to the gastric bypass patients. Study participants were enrolled under the Helsinki Declaration and provided written informed consent. The studies were approved by the Swedish Ethical Review Authority (682-14, 2019-04046) and registered with ClinicalTrials.gov (NCT02322073, NCT04255264).

Categorizing responders vs. non-responders

Patient-specific adipose explants taken from the greater omentum were treated with lipoxins *ex vivo*. Approximately 50% of explant cultures responded to the treatment by significantly upregulating the M2 macrophage marker CD206. The switch from an M1 to the M2 macrophage phenotype has been established as a lipoxin-mediated response (Börgeson et al., 2015). Manual screening of the participants' routinely collected clinical values revealed that all responders had mildly elevated CRP levels (defined by the Sahlgrenska University Hospital as ≥5 mg/L). In contrast, the non-responders had low CRP levels, which was thus used as the clinical criterion to separate the groups.

METHOD DETAILS

Clinical blood analyses

Venous blood was collected in K_2EDTA (Greiner Bio One) tubes and sent to the hospital's accredited laboratory services to analyze liver function (ALT, AST, ALP), hyperlipidemia (Cholesterol, Triglycerides, HDL, LDL) and clinically used inflammatory markers (white blood cell count, CRP), as reported in Table 1. Of note,

the limit of detection when measuring CRP is 1 mg/L. Healthy individuals, such as the control group, will fall below the limit of detection and for these individuals the CRP levels are reported as 1.0 mg/L, as per common clinical practice.

Plasma protein screen

Venous blood was collected in K_2EDTA (Greiner Bio One) tubes after an overnight fast. Plasma was prepared through centrifugation and stored at −80°C until analysis. Protein biomarkers were analyzed by Olink proximity extension assay for inflammatory proteins (Olink Proteomics, Uppsala, Sweden) at the Clinical Biomarkers Facility at Science for Life Laboratory (Uppsala University, Sweden). To avoid intra-assay variability, samples were analyzed on the same plate (Rajan et al., 2019). Briefly, proteins with <30% missing values in at least one of the groups were analyzed (Figure S2). For the proteins that met these criteria, missing values were replaced with limit of detection (LOD) values, per the manufacturer's recommendation. We confirmed that the dataset did not include outliers using hierarchical clustering with Pearson correlation distance and complete linkage. Concentrations of proteins are reported as normalized protein expression (NPX) values, an arbitrary unit on a $\log_2$ scale.

Adipose tissue explant culture

Adipose tissue was collected from the greater omentum in connection with the patient's gastric bypass surgery. The tissue was rinsed in saline, and larger blood vessels were dissected away. The tissue was divided into 0.5 g explants and incubated with serum free DMEM media supplemented with vehicle (0.1% ethanol), LXA_4 (1 nM) or LXB_4 (1 nM) at 37°C for 6 hours. Subsequently, the tissue was collected and rinsed in saline prior to snap freezing for further analyses. The supernatants were cleared of cellular debris by centrifugation (1000*g*, 10 min, 4°C) and snap frozen.

Immunofluorescence

Omental adipose tissue was paraffin embedded, sectioned and stained (Soták et al., 2021). Briefly, deparaffinized sections were antigen retrieved by boiling sections in a pressure cooker (Antigen Retriever 2100) for 20 min in antigen retrieval buffer (0.05% Tween-20, 10 mM Citrate unmasking buffer, pH 6.0 for FPR2 staining and 0.05% Tween-20, 1 mM EDTA, 10 mM Tris, pH 9.0 for CD68/CD206/CD11c staining). The sections were left to cool for 1.5 hours and subsequently rinsed three times using PBS. The sections were permeabilized for 10 min in 0.5% Triton X-100 (Sigma) in PBS before blocking for 2 hours at room temperature using 3% BSA (Sigma), 3% donkey serum (Sigma), and 0.3M glycine (Sigma) in PBS. Following blocking, sections were incubated with antibodies directed against either FPR2 (Anti-FPR2 antibody, Novusbio, NLS1878 lot#A8), CD68 (Anti-CD68 antibody [EPR20545], Abcam, ab213363), CD206 (Human MMR/CD206 antibody, R&D, AF2534) or CD11c (Anti-CD11c antibody [ITGAX/1243], Abcam, ab215858) at 4°C overnight, followed by three 5 min washes using 0.1% Triton-X100 in PBS. Subsequently, sections were incubated with secondary antibodies (Alexa Fluor 488 Donkey Anti-Rabbit antibody, Alexa Fluor 594 Donkey Anti-Mouse antibody, Cy5 Donkey Anti-Goat antibody, Jackson Immuno Research) and DAPI (4′,6-Diamidino-2-Phenylindole, Dihydrochloride, Thermo Fisher) for 1 hour at room temperature, followed by three 5 min washes of 0.1% Triton X-100 in PBS and a 30 second incubation with TrueBlack (VWR) to quench lipofuscin autofluorescence. Sections were embedded using Prolong Gold mounting media (Thermo Fisher) and imaged using a Nikon Eclipse E400 (Nikon, Tokyo, Japan) microscope equipped with a Plan 10x/0.25 lens as well as DAPI (340–380 nm) and FITC (465–495 nm) filters. Image acquisition and analysis were completed using ACT-1 (Nikon) and Fiji (ImageJ, NIH). Image analysis using CellProfiler (Broad Institute) was used for the quantification of colocalization between CD68 and either CD11c or CD206 positive cells in immunofluorescently stained sections of adipose tissue explants.

Cell isolation from human adipose tissue

Human subcutaneous adipose tissue was dissected and minced. The tissue was digested at 37°C for 45 min with agitation in digestion buffer 1 mg/mL type 2 collagenase (Worthington, LS004177) in HBSS buffer, pH 7.4, supplemented with 2% BSA. The cell suspension was subsequently filtered through a sterile 250 μm mesh filter to remove undigested tissue, after which floating mature adipocytes were isolated via floating for culture. Meanwhile, the adipose stroma vascular fraction (SVF) was pelleted through centrifugation (200*g*, 7 min at room temperature) and used for experiments as described below. Additionally, the mature floating adipocytes were washed three times in KRHB wash buffer (120 mM NaCl, 4.7 mM KCl, 1.2 mM KH_2PO_4, 1.2 mM $MgSO_4 \cdot 7\ H_2O$, 2.5 mM $CaCl_2 \cdot 2\ H_2O$, 25 mM HEPES, 2 mM glucose, 2% BSA, pH 7.4)

using a separation funnel (VWR) to ensure removal of any remaining collagenase, leaving the mature adipocytes to be cultured as described in the MAAC procedure below (Alexandersson et al., 2020; Harms et al., 2019).

Membrane mature adipocyte aggregate culture (MAAC) model

Isolated mature floating adipocytes were centrifuged (50*g*, 3 min, room temperature) to separate and aspirate any remaining wash buffer from the adipocytes. Any visible free lipid layer on top of the mature adipocytes (i.e., oil from adipocytes that may have ruptured during the isolation procedure) was removed. Subsequently, the mature adipocytes were seeded onto upside-down turned transwell insert, then inverted into tissue culture media in 24-well plate (DMEM containing 3% FBS, 1% Penicillin/Streptomycin) (Figure 1A). The cells were allowed to recover overnight before being treated with vehicle (0.1% ethanol), LXA_4 (1 nM) or LXB_4 (1 nM) for four days. Media was subsequently removed and cleared by centrifugation (1000*g*, 10 min, 4°C) before being snap frozen for downstream analyses. The remaining cells were harvested in 500 μL Trizol (Invitrogen) for subsequent RNA isolation and quantifying gene expression.

Differentiated human adipocyte culture

The SVF (containing adipocyte precursors, endothelial cells, immune cells, etc.) underwent an erythrocyte lysis step (Invitrogen) for 5 min at room temperature. Following additional centrifugation (518*g*, 10 min at room temperature) and washing steps in subcutaneous basal medium (ZenBio), cells were seeded at the density between 20,000–25,000 cells/cm^2 in a cell factory and expanded in the presence of bFGF (0.17 ng/mL). The resulting cell population was subsequently referred to as pre-adipocytes and were seeded for experimental use at a density of 37,500 cells/cm^2 in subcutaneous basal medium (ZenBio), 3% FBS (Hyclone), 1% Penicillin/Streptomycin (CellGro), 1nM bFGF (Sigma) in 24-well plates. Cells were differentiated one-day post confluence (differentiation Day 1) in basal medium (Zenbio) with 3% FBS (Hyclone), 1% Penicillin/Streptomycin (CellGro), 1 μM pioglitazone (Sigma), 0.5 mM IBMX (Sigma), 1 μM dexamethasone (Sigma) and 100nM insulin (Novo Nordisk). On day 8 of differentiation, the medium was changed to the same media as above, but without pioglitazone, dexamethasone or IBMX. Differentiated adipocytes were treated with vehicle (0.1% ethanol), LXA_4 (1 nM) or LXB_4 (1 nM) for four days. Cells were harvested in RLT Buffer (Qiagen RNeasy mini kit cat# 74106) to isolate total RNA, while supernatants were collected and snap frozen for further downstream analyses. Supernatant cytokine production was determined by standard enzyme-linked immunosorbent assay (ELISA) or Meso Scale Discovery (MSD) platform analyses.

Human unilocular vascularized adipocyte spheroid (HUVAS) cultures

Human subcutaneous adipocyte spheroids were cultured as described (Ioannidou et al., 2021). Briefly, primary human subcutaneous SVF cells (including pre-adipocytes, endothelial cells and immune cells) from a healthy female donor (Lonza, US) were seeded in a 96-well ultra-low attachment plate (Corning) at a concentration of 10,000 cells per well in Endothelial growth medium 2 (Lonza). On day 6, the formed spheroids were embedded in 40 μL of growth factor-reduced Matrigel (Corning) to allow vascular sprouting. On day 10, half of the cell culture media was replaced with twice as concentrated Preadipocyte Growth Medium (PGM-2, Lonza) to induce adipocyte differentiation. New PGM-2 media was added on day 15 and day 26. Cells were then treated with vehicle (0.1% ethanol), LXA_4 (1 nM) or LXB_4 (1 nM) for 4 days, after which the culture media was collected and snap frozen. The spheroids were briefly washed in PBS, and each spheroid was subsequently homogenized in 100 μL Qiazol (Qiagen) by centrifuging them twice through a QIAshredder column (Qiagen).

Gene expression analyses

Adipose tissue was homogenized in Trizol (100 mg/mL), and after centrifugation, the aqueous phase was transferred to an RNeasy Mini Kit (Qiagen) column, and RNA was isolated according to the manufacturer's instructions. RNA concentration and purity were assessed using NanoDrop 2000 (Thermo Fisher Scientific), and RNA integrity was verified by RNA Pico Chip using an Agilent 2100 Bioanalyzer (Agilent Technologies, Germany). RNA samples were treated with DNAse I (Invitrogen) and cDNA synthesized using random hexamers and Superscript IV (Invitrogen) according to the manufacturer's instructions. mRNA expression was evaluated by droplet digital PCR (ddPCR) on a QX200 AutoDG Droplet Digital PCR System (Bio-Rad). Two reference internal control genes (*LRP10*, *RPLP0*), previously shown to be stably expressed in human adipose

tissue (Gabrielsson et al., 2005), were used to generate a normalization factor, which was calculated as a geometric mean normalized to maximal values (Vandesompele et al., 2002).

RNA samples from female obese patients that were grouped into the responding or non-responding groups were analyzed by RNA-Seq next generation sequencing by SNP&SEQ Technology Platform (Uppsala, Sweden). Please note that transcriptome analysis has not been performed on male patient omental white adipose tissue biopsies owing to the low number of available samples. The sequencing library was prepared using accredited method of TruSeq stranded mRNA library preparation kit with polyA selection (Illumina, San Diego, CA). 150 cycles paired-end sequencing were performed using the NovaSeq 6000 system and v1 sequencing chemistry (Illumina) aiming for average coverage of 30 M reads per sample. The quality of reads was examined using MultiQC (Ewels et al., 2016) and sequences were further aligned using STAR (Dobin et al., 2012) and read count summarized using featureCounts (Liao et al., 2013). DeSeq2 package (Love et al., 2014) in R environment v. 4.1.0 (https://www.R-project.org/) was used to assess differentially expressed genes. FDR correction was applied to adjust p values and comparisons with $\log_2$ fold change >0.5 and $p < 0.1$ were considered significant.

Targeted lipidomics analyses

Adipose tissue non-esterified oxylipins, endocannabinoids, and ceramides were isolated and quantified using modifications of published protocols (Bielawski et al., 2006; Midtbo et al., 2015; Pedersen and Newman, 2018). Briefly, ~30 mg of frozen tissue was spiked with deuterated oxylipin, endocannabinoid and ceramide surrogates, mixed with butylated hydroxyl toluene and ethylene diamine tetraacetic acid. The sample was then homogenized in 400 μL of isopropanol containing the internal standards 1-cyclohexyl ureido, 3-dodecanoic acid and 1-phenyl ureido 3-hexanoic acid using three 3 mm steel beads and shaking on a Geno/Grinder 2010 (SpeX SamplePrep, Metuchen, NJ). Protein precipitate and debris were removed by centrifugation for 10 min at 10,000*g* and 6°C, followed by 10 min at 15,000 *g* at 4°C. Extracts were diluted 1:1 with acetonitrile for oxylipin and endocannabinoid analyses, or 1:10 with isopropanol for ceramide analyses. Diluted samples were stored at −20°C until analysis.

Analytes were separated using a Waters Acquity ultra-performance liquid chromatography (UPLC; Waters, Milford, MA) on a 2.1 mm × 150 mm, 1.7 μm BEH C18 column (Waters) for analysis of oxylipins and endocannabinoids, and 2.1 mm × 150 mm, 1.7 μm BEH C8 column (Waters) for analysis of ceramides. Separated analytes were detected using tandem mass-spectrometry, using electrospray ionization with multi reaction monitoring on an API 6500 QTRAP (Sciex, Redwood City, CA) for oxylipins and endocannabinoids, and an API 4000 QTRAP (Sciex) for ceramides. Analytes were quantified using internal standard methods and 7-9 point calibration curves of authentic standards (Agrawal et al., 2018).

QUANTIFICATION AND STATISTICAL ANALYSIS

Data were analyzed using R (http://www.R-project.org/, version 4.1.0), Excel (Microsoft, version 16.54) and GraphPad Prism (GraphPad Software Inc., version 8). Data obtained from human tissues were presumed to have a non-Gaussian distribution, and thus statistical significance ($p < 0.05$) for continuous variables was determined using Mann-Whitney U test when comparing two groups. Kruskal-Wallis with Dunn's post-hoc tests were used when comparing more than two groups, unless the data was presented on a logarithmic scale at which point a parametric analysis of ANOVA with Fisher's least significant difference post-hoc test was performed. Clinical categorical variables were analyzed using Fisher's exact test. Analyses of experiments using the uniformly cultured cell-line were assumed to have a Gaussian distribution, and thus significance ($p < 0.05$) was determined using a Student's t-test when comparing two groups, and ANOVA with the least significant difference post-hoc comparison tests when comparing more than two groups. Data are presented as mean ± standard error of the mean (SEM) or median ± interquartile range (IQR), *$p < 0.05$, **$p < 0.01$, ***$p < 0.001$, as also stated in respective figure or table legend. Data from cell-culture experiments are presented as bar-graphs, while patient-related data is presented as box and whisker plots.

ADDITIONAL RESOURCES

Prior to enrolling participants, the studies were approved by the Swedish Ethical Review Authority (682-14, 2019-04046) and registered with ClinicalTrials.gov (NCT02322073, NCT04255264).